Manuscript prepared for Earth Syst. Dynam.
with version 5.0 of the LaTeX class copernicus.cls.
Date: 20 March 2014

Supplement for
Global and regional effects of land-use change on climate in 21st century simulations with interactive carbon cycle

L. R. Boysen[1,*], V. Brovkin[1], V. K. Arora[2], P. Cadule[3], N. de Noblet-Ducoudré[3], E. Kato[4], J. Pongratz[1], and V. Gayler[1]

[1]Max Planck Institute for Meteorology, Hamburg, Germany
[2]Canadian Centre for Climate Modelling and Analysis, Environment Canada, University of Victoria, British Columbia, Canada
[3]Laboratoire des Sciences du Climatet de l'Environnement, Gif-sur-Yvette, France
[4]National Institute for Environmental Studies, Tsukuba, Japan
[*]Now at: Potsdam Institute for Climate Impact Research, Research Domain 1: Earth System Analysis, Telegraphenberg A62, 14473 Potsdam, Germany, E-mail: lboysen@pik-potsdam.de

Correspondence to: L. R. Boysen
(lboysen@pik-potsdam.de)

1 Model specifications and LULCC implementation

The implementation of LULCC patterns is approached differently among the models (see table S1). Two of the analyzed models, MPI and MIR, implement a transition matrix of annual fractional changes within each grid cell into their dynamic vegetation models. The consequences are possible multiple conversions within individual grid cells, which might actually not be seen in changes of the grid cell's net land cover distribution but in the allocation of carbon between the different pools. CAN and IPSL do not model dynamic vegetation and thus, exclude vegetation shifts due to climatic changes. Anthropogenic pastures are excluded in CAN and IPSL simulates increases in grassland whenever an increase in grazing land is required by the LULCC scenario. This has consequences for the comparison of these areas among the models as MPI and MIR-LR both assume that pastures are not affected by fires, resulting into larger areas. CAN is the only model that simulates cropland explicitly whereas the other models treat crops as grassland but specifications are made: MPI and IPSL use a modified phenology, MPI simulates crops with a higher albedo and MIR implements annual crop harvest. The spread between models with and without dynamic vegetation is visible with respect to the area altered by LULCC in 2100 compared to 2006 (figure S1): CAN and IPSL simulate a net change of cultivated area of 2.7 and 2.3 x 10^6 km^2, respectively. MIR and MPI apply dynamic vegetation models which are capable of accounting for pastures, regrowth and abandonment and thus result in the strongest increases of 5.4 x 10^6 km^2 and 8.2 x 10^6 km^2, respectively. A detailed description on the participating models, the implementation of land-use maps and the land harmonization project can be found in the analysis of Brovkin et al. (2013).

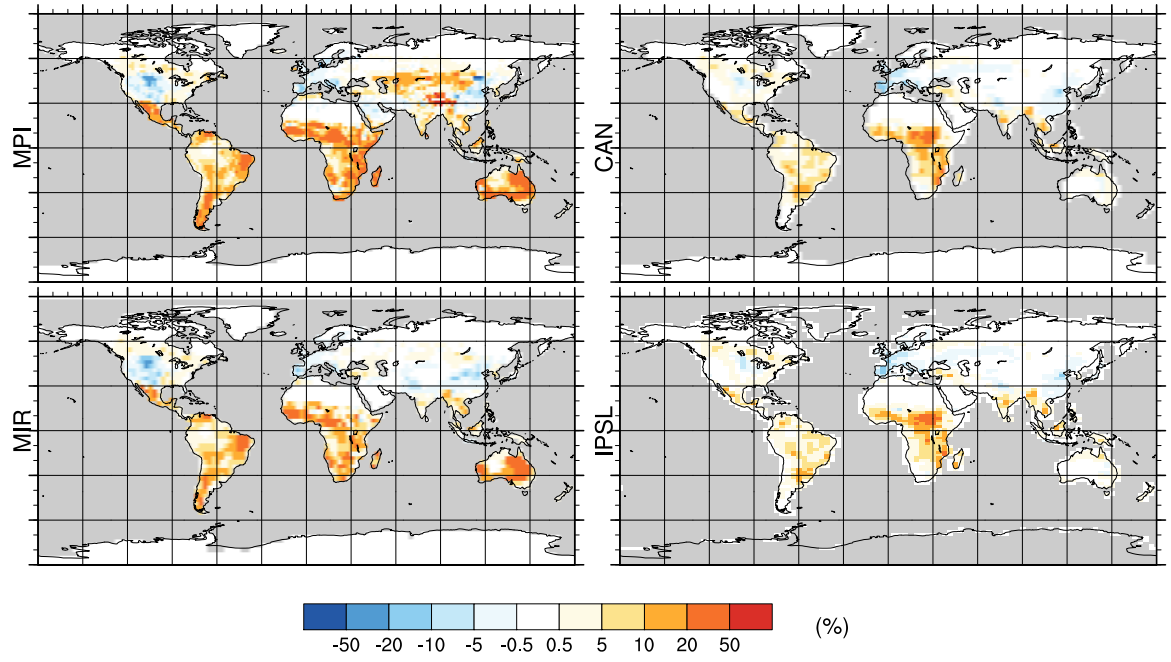

Fig. S1. Maps displaying the change in agricultural area (crops and pastures; % of grid cell area) in 2100 compared to 2006 for the four Earth System models.

Table S1. Brief description of models participating in the LUCID-CMIP5 simulations (following Brovkin et al., 2013). ESM references are: CAN Arora et al. (2011), IPSL Dufresne et al. (2013), MIR Watanabe et al. (2011) and MPI Giorgetta et al. (2012) and Reick et al. (2013).

ESM	CAN	IPSL	MIR	MPI
Atmosphere/land resolution	≈2.8°	3.75°x 1.90°	≈2.8° (T42)	≈1.9° (T63)
Land surface component	CTEM	ORCHIDEE	SEIB-DGVM	JSBACH
Number of PFTs	9	13	13	12
Dynamic vegetation	No	No	Yes	Yes
Fire module	No	Yes	No	Yes
Crop PFT	Yes	Yes	No[a]	No[b]
Pastures	No	No[c]	Yes	Yes
Wood harvest	No	No	No	Yes
Usage of land-use transitions Hurtt et al. (2011)	No	No	Yes	Yes

[a] Uses grasses' PFT parameters for crops, but harvested annually.

[b] Crops differ from grasses in parameters pf photosynthesis and phenology.

[c] Simulates grasses where pastures grow.

2 Supplementary material on CO_2 and near-surface temperature in section 3.1.

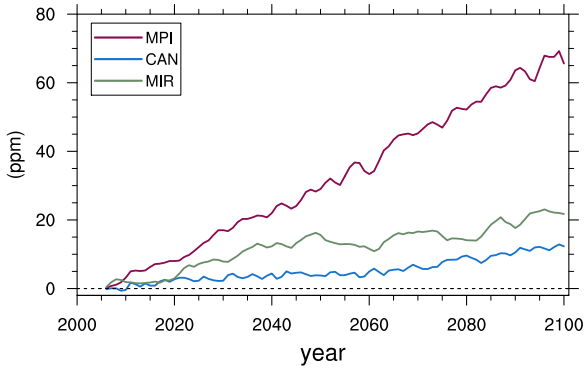

Fig. S2. Effect of LULCC on the annual global mean atmospheric CO_2 concentration (ppm).

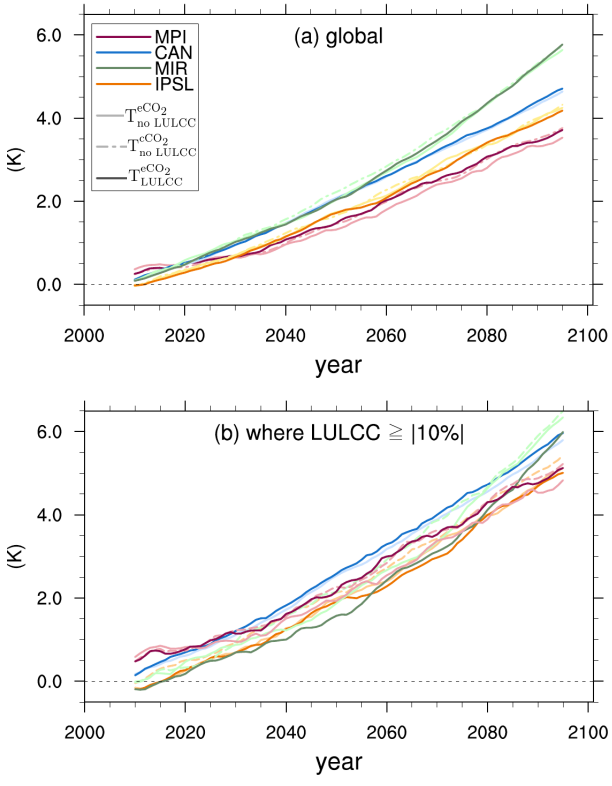

Fig. S3. 10-years running mean of global annual near-surface temperatures across all models relative to 2006 values (in K). (a) global values; (b) values averaged only over areas where LULCC $\geq 10\%$ of the grid cell in 2100 compared to 2006. Dark solid lines represent the $T^{eCO_2}_{noLULCC}$ run, light solid lines the $C^{eCO_2}_{noLULCC}$ simulation and dashed lines mark the $T^{cCO_2}_{noLULCC}$ scenario.

Table S2. Values depicted in figure 2. Relative changes in near-surface temperature: Comparison of $\Delta_t T_{BGP}$ relative to $\Delta_t T^{cCO_2}_{noLULCC}$, that is the BGP impacts of LULCC compared to the impacts of anthropogenic carbon emissions (both fossil-fuel and LULCC, L1A simulation) on near-surface temperature (in %). Depicted are mean 2071-2100 values minus the 2006 state (indicated by "Δ_t"). Positive (negative) values indicate that BGP effects ($\Delta_t T_{BGP}$) enhance (dampen) the change caused by LULCC and other anthropogenic emissions. Analysis is done for the following regions: Eurasia (EURA), North America (NOAM), South America (SOAM), Africa (AFRI), Australia (AUST), land (land area) and global (total area on Earth). Values without, with (*) and with two (**) asterisks exceed the statistical significance at the 95%, 90% and 80% level, respectively.

	region	$\Delta_t T^{cCO_2}_{noLULCC}$ (K)	$\Delta_t T^{eCO_2}_{LULCC}$ (K)	$\Delta_t T_{BGP}$ (K)	rel. change (%)
MPI	EURA	4.36	4.30	(-0.06**)	-1
	NOAM	5.02	4.69	-0.33	-6
	SOAM	4.48	4.89	0.40	9
	AFRI	4.68	4.80	(0.12)	3
	AUST	5.25	4.66	-0.58	-11
	land	4.59	4.49	(-0.10)	-2
	global	3.25	3.25	(0.01)	0
MIR	EURA	7.28	7.40	(0.12**)	2
	NOAM	7.70	7.83	(0.12**)	2
	SOAM	5.61	5.40	-0.21	-4
	AFRI	5.31	4.86	-0.45	-8
	AUST	5.47	4.22	-1.25	-23
	land	6.53	6.42	(-0.11*)	-2
	global	4.85	4.82	(-0.03)	-1
IPSL	EURA	5.34	5.44	(0.10**)	2
	NOAM	4.64	4.92	0.10	6
	SOAM	4.61	4.12	-0.49	-11
	AFRI	5.15	4.63	-0.52	-10
	AUST	4.21	4.29	(0.08)	2
	land	4.63	4.52	-0.11	-2
	global	3.68	3.63	(-0.05**)	-1

3 Supplementary material on carbon fluxes in section 3.3. and 3.4

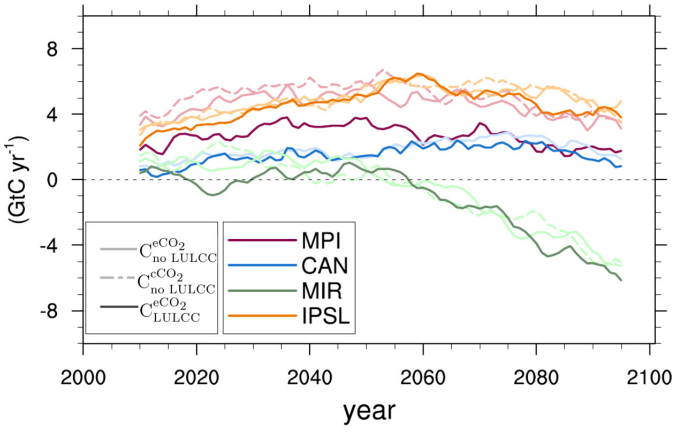

Fig. S4. Global 10-years-running mean of annual land carbon uptake (in $\mathrm{GtC\,yr^{-1}}$).

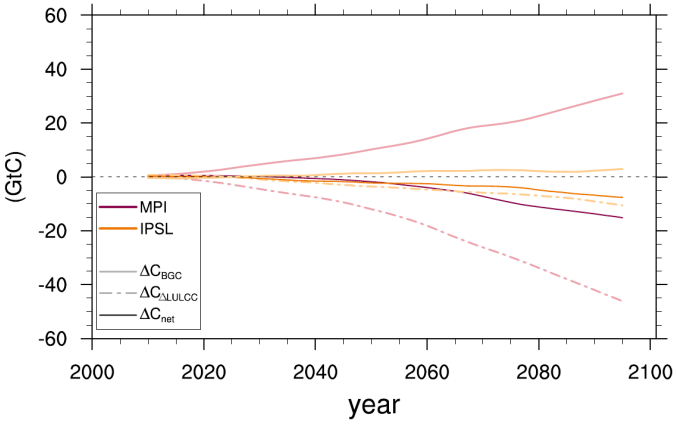

Fig. S5. 10-years-running global means of net changes due to LULCC in cumulative fire emissions of ESM runs (in GtC).

References

Arora, V., Scinocca, J., Boer, G., Christian, J., Denman, K., Flato, G., Kharin, V., Lee, W., and Merryfield, W.: Carbon emission limits required to satisfy future representative concentration pathways of greenhouse gases, Geophysical Research Letters, 38, L05 805, 2011.

Brovkin, V., Boysen, L., Arora, V., Boisier, J., Cadule, P., Chini, L., Claussen, M., Friedlingstein, P., Gayler, V., van den Hurk, B., Hurtt, G., Jones, C., Kato, E., de Noblet Ducoudré, N., Pacifico, F., Pongratz, J., and Weiss, M.: Effect of anthropogenic land-use and land cover changes on climate and land carbon storage in CMIP5 projections for the 21st century., Journal of Climate, doi:10.1175/JCLI-D-12-00623.1, http://dx.doi.org/10.1175/JCLI-D-12-00623.1, 2013.

Dufresne, J.-L., Foujols, M.-A., Denvil, S., Caubel, A., Marti, O., Aumont, O., Balkanski, Y., Bekki, S., Bellenger, H., Benshila, R., et al.: Climate change projections using the IPSL-CM5 Earth System Model: from CMIP3 to CMIP5, Climate Dynamics, pp. 1–43, 2013.

Giorgetta, M., Jungclaus, J., Reick, C., Stevens, B., Marotzke, J., Claussen, M., Roeckner, E., Mauritsen, T., Crueger, T., Schmidt, H., et al.: Climate variability and climate change in MPI-ESM CMIP5 simulations, J. Adv. Model. Earth Syst., in revision, 2012.

Hurtt, G., Chini, L., Frolking, S., Betts, R., Feddema, J., Fischer, G., Fisk, J., Hibbard, K., Houghton, R., Janetos, A., et al.: Harmonization of land-use scenarios for the period 1500–2100: 600 years of global gridded annual land-use transitions, wood harvest, and resulting secondary lands, Climatic Change, pp. 1–45, 2011.

Reick, C., Raddatz, T., Brovkin, V., and Gayler, V.: The representation of natural and anthropogenic land cover change in MPI-ESM, Journal of Advances in Modeling Earth Systems, 2013.

Watanabe, S., Hajima, T., Sudo, K., Nagashima, T., Takemura, T., Okajima, H., Nozawa, T., Kawase, H., Abe, M., Yokohata, T., et al.: MIROC-ESM 2010: model description and basic results of CMIP5-20c3m experiments, Geoscientific Model Development, 4, 845–872, 2011.